J. Fluid Mech. (1982), *vol.* 118, *pp.* 445–470
Printed in Great Britain

Measurement of fluid turbulence based on pulsed ultrasound techniques. Part 1. Analysis

By JOSEPH L. GARBINI, FRED K. FORSTER† AND JENS E. JORGENSEN

Department of Mechanical Engineering,
University of Washington, Seattle, U.S.A.

(Received 27 February 1981 and in revised form 30 September 1981)

The pulsed ultrasonic Doppler velocimeter has been used extensively in transcutaneous measurement of the velocity of blood in the human body. It would be useful to evaluate turbulent flow with this device in both medical and non-medical applications. However, the complex behaviour and limitations of the pulsed Doppler velocimeter when applied to random flow have not yet been fully investigated.

In this study a three-dimensional stochastic model of the pulsed ultrasonic Doppler velocimeter for the case of a highly focused and damped transducer and isotropic turbulence is presented. The analysis predicts the correlation and spectral functions of the Doppler signal and the detected velocity signal. The analysis addresses specifically the considerations and limitations of measuring turbulent intensities and one-dimensional velocity spectra.

Results show that the turbulent intensity can be deduced from the broadening of the spectrum of the Doppler signal and a mathematical description of the effective sample-volume directivity.

In the measurement of one-dimensional velocity spectra at least two major complications are identified and quantified. First, the presence of a time-varying, broad-band random process (the Doppler ambiguity process) obscures the spectrum of the random velocity. This phenomenon is similar to that occurring in laser anemometry, but the ratio of the level of the ambiguity spectrum to the largest detected velocity spectral component can be typically two to three orders of magnitude greater for ultrasonic technique owing to the much greater wavelength.

Secondly, the spatial averaging of the velocity field in the sample volume causes attenuation in the measured velocity spectrum. For the ultrasonic velocimeter, this effect is very significant.

The influence of the Doppler ambiguity process can be reduced by the use of two sample volumes on the same acoustic beam. The signals from the two sample volumes are cross-correlated, removing the Doppler ambiguity process, while retaining the random velocity. The effects of this technique on the detected velocity spectrum are quantified explicitly in the analysis for the case of a three-dimensional Gaussian-shaped sample-volume directivity.

---

† Also at Center for Bioengineering, University of Washington, Seattle.

1. Introduction

1.1. *Preliminary remarks*

Pulsed ultrasonic Doppler velocimetry combines the transmission of bursts of high-frequency sound with the gated reception of the scattered acoustic energy to measure velocity at a specific point in a flowing liquid. The potential exists for the use of this device in circumstances where it is impracticable to invade the flow field or where ultrasound offers advantages over the use of thermal or laser anemometry. Liquids containing particulates, sediments or gas bubbles complicate the use of hot-film probes but may provide ideal conditions for acoustic measurements. For example, in employing thermal anemometry to measure turbulence in the ocean a major problem is physical protection and cleaning of the sensing element. These problems would be virtually non-existent for an ultrasonic velocimeter.

The primary aim of this study is to evaluate the conditions under which velocity correlations or velocity spectra may be measured with ultrasonic Doppler velocimetry. Towards this end, an analytical model of this instrument for homogeneous turbulence in steady flow has been developed, and the limitations in measurement accuracy and resolution are explored.

The Doppler ambiguity process, similar to but generally more restricting than that of laser instruments, poses a major limitation to ultrasonic velocimetry. A dual-measurement technique for reducing the effective Doppler ambiguity, which takes advantage of the pulsed nature of this instrument, is proposed and its efficiency examined.

In addition, an extensive laboratory experimental programme was undertaken to examine the validity of all major model implications and to evaluate the Doppler ambiguity reduction technique. The results of the experimental investigation are presented in part 2 of this study (Garbini, Forster & Jorgensen 1982).

1.2. *Pulsed ultrasonic Doppler flowmeter principles*

The pulsed ultrasonic Doppler velocimeter (PUDV) to be considered in this study is of a type commonly used for medical diagnosis. It employs a single piezoelectrical crystal transducer for both transmitting and receiving acoustic signals. The transducer is focused to a narrow beam at a distance of 2 to 10 cm. The transmitted signal is composed of bursts of a high-frequency sinusoid which are regularly repeated at a much lower frequency. Typical values of the master oscillator frequencies are 1–10 MHz and those of the pulse repetition frequency (PRF) are 5–30 kHz. Between transmitted bursts the receiver is activated to detect echoes from particles in the flow. This signal contains the superposition of echoes from the particles within the ultrasonic beam. Since the particles are moving, each scattered echo is Doppler-shifted in frequency.

The received signal is mixed with (multiplied by, in this context) a continuous sinusoid with frequency equal to that of the master oscillator. High-frequency components are filtered from the resulting waveform, leading only components of frequency equal to the difference between the master oscillator frequency and that of the received signal, i.e. the Doppler frequency.

The output of the mixer is continuously sampled at the PRF but at times delayed by τ with respect to the transmission of the bursts. The echoes sampled at these

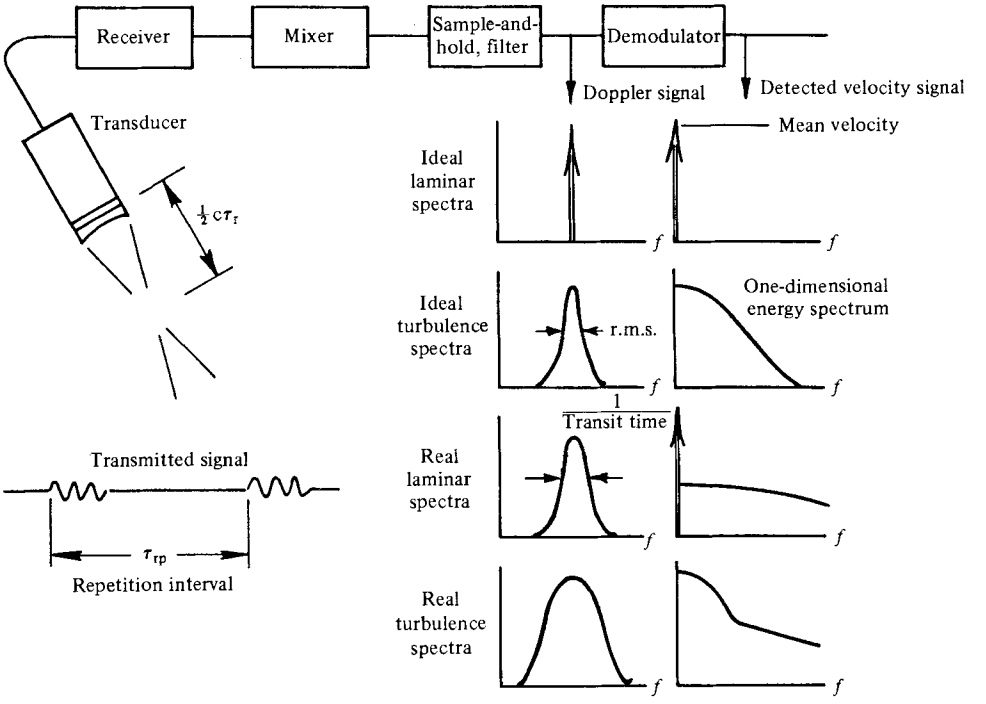

FIGURE 1. Operation of the pulsed ultrasonic Doppler velocimeter.

distances can only have originated in regions in space that are located at multiples of $\frac{1}{2}\tau c$. Further, the axial dimension of these regions must correspond to the equivalent spatial length of a transmitted burst. Normally, proper experimental design and attenuation in the acoustic medium ensure that only echoes from the nearest of these regions will contribute significantly to the result. This region in space is commonly called the sample volume. It is described by a spatial weighting function characterized in the lateral beam direction by the sound field, and in the axial direction by the shape of the transmitted burst.

The sampled signal is then filtered to produce an analog waveform called the Doppler signal. Ideally, the frequency of the Doppler signal is proportional to the velocity of the particles within the sample volume. This is described by the formula

$$f_d = \frac{2f_0 V}{c} \cos\theta, \tag{1.1}$$

where f_d is the Doppler signal frequency, f_0 is the master oscillator frequency, c is the speed of sound, V is the speed of the particles, and θ is the angle between the ultrasonic beam and the direction of motion (the Doppler angle).

The Doppler signal frequency can be measured in a manner similar to FM demodulation to obtain a direct measure of the velocity. However, the resulting output contains additional components that are not related directly to velocity. Therefore this quantity is referred to as the detected velocity signal.

For both laminar and turbulent flow, the output of the pulsed ultrasonic Doppler velocimeter may be considered in terms of the power spectra of the Doppler and detected velocity signals. In a highly idealized sense these cases are depicted in the top

four graphs of figure 1. Significant to this discussion is that the spectrum of the detected velocity signal is associated (§ 2.3) with the one-dimensional energy spectrum of turbulent flow. Also, the width of the Doppler signal spectrum is related to the turbulence intensity (§ 2.2).

The description, so far, of the ultrasonic velocimeter has been highly simplified. Effects associated with the site and shape of the sample volume and with the detection process contribute to deviations from these concepts. For instance, in the relatively simple case of laminar flow the random transit of particles through the finite sample volume will cause the Doppler signal spectrum to broaden. This causes a broad-band noise process to be introduced into the Doppler velocity spectrum.

For turbulent flow, this same phenomenon increases the width of the Doppler spectrum beyond that associated with the turbulence intensity. In turn, the one-dimensional energy spectrum estimate is contaminated by the superposition of the broad-band noise process.

This 'transit-time' effect, which is illustrated in the bottom four graphs of figure 1, will be analysed in detail, along with other characteristics of the ultrasonic velocimeter, in § 2.

2. Analysis

2.1. *The Doppler signal*

Although stochastic models for ultrasonic Doppler velocimeters are described in the literature (Brody & Meindl 1974; Flax, Webster & Stuart 1971; Newhouse 1973), they apply primarily to situations in which the flow is steady and laminar. Very little consideration has yet been given to the characteristics of the devices in either non-steady or turbulent flows. Further, the existing models do not apply precisely to the type of instrument described here.

The following analysis of the pulsed ultrasonic Doppler velocimeter is intended to apply to the high-resolution system described in § 1. It is assumed that the device uses a single-crystal transducer, coherent demodulation, and sample-and-hold gating. While major considerations, assumptions and results are presented here, a more detailed derivation may be found in the literature (Garbini 1978).

Consider the situation of a single particle within the range of the transducer satisfying the following assumptions.

(i) The particle diameter is small with respect to the wavelength, λ, of the transmitted acoustic carrier.

(ii) Acoustic scattering from the particle has random amplitude and phase.

(iii) The component of the particle velocity in the direction of the transducer is much smaller than the speed of sound in the fluid medium. Also, the average value of this component is much greater than the velocity fluctuations.

(iv) The effective ultrasonic beam length is shorter than the unambiguous range ($\frac{1}{2}c\tau_{rp}$, where τ_{rp} is the pulse-repetition interval). This ensures that only information from a single spatial sample volume nearest to the transducer is processed.

(v) The sampling region is sufficiently small and distant from the transducer that the distance from a particle in the same volume to any point on the transducer is constant. This is approximately true for particles in the far field of acoustically focused transducers.

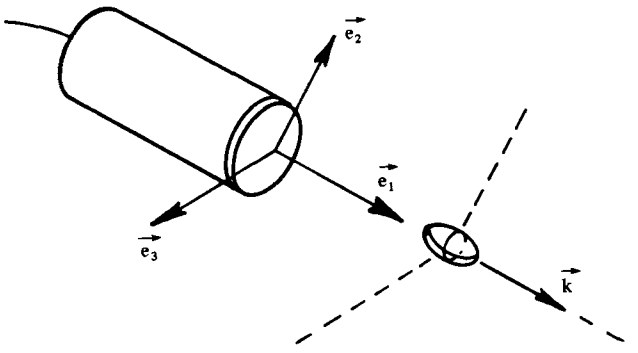

FIGURE 2. The co-ordinate system.

(vi) The transmitted signal consists of a high-frequency carrier modulated by a periodically repeated envelope function that varies slowly in comparison with the carrier. That is

$$x_t(t) = \text{const.} \times \sum_{n=-\infty}^{+\infty} F(t - n\tau_{rp}) \cos \omega_0 (t - n\tau_{rp}), \tag{2.1}$$

where F is the envelope function describing the pulse shape, and ω_0 is the radian frequency of the carrier.

Under these conditions the sampled output of the mixer is

$$x_s(t) = \text{const.} \times \left[\sum_{n=-\infty}^{+\infty} \delta(t - n\tau_{rp} - \tau_r) \right] aH(\tau) \cos(\mathbf{k} \,.\, \mathbf{r} + \gamma), \tag{2.2}$$

where τ_r is the range delay interval, $\mathbf{r}$ is the position vector of the particle, δ is the delta function, a is the random scattering amplitude, γ is the random scattering phase, and $\mathbf{k}$ is the sum of the transmitted and received wave vectors. The distance to the sample volume is $\frac{1}{2}\tau_r c$.

For the case of a single-crystal transducer, $\mathbf{k}$ points straight out from the transducer and has magnitude $2\omega_0/c$. $H(\mathbf{r})$ is the effective sample-volume directivity function. It is proportional to the product of the combined transmitting and receiving directivities, and the shifted envelope function, $F(t - \mathbf{r} \,.\, \mathbf{k}/\omega_0)$; see figure 2.

In this development the absolute magnitude of the back-scattered amplitude is not of direct importance. Therefore, here, and throughout the remainder of this discussion $H(\mathbf{r})$ is normalized such that

$$\int_{\text{space}} H(r)\, d\mathbf{r} = 1, \tag{2.3}$$

and a constant factor will be carried along, as in (2.2). The position of the particle may be expressed in terms of its initial position, $\mathbf{r}^0$, plus the integral of its velocity. That is

$$\mathbf{r}(t) = \mathbf{r}^0 + \int_0^t \mathbf{U}(\xi)\, d\xi. \tag{2.4}$$

In general, the sample volume will contain many particles. In the following analysis it will be seen that the effective velocity observed by the flowmeter corresponds to

the average of the individual velocities, weighted by the sample-volume directivity function

$$\langle \mathbf{u} \rangle (t) = \frac{1}{N} \sum_{i=1}^{N} H(\mathbf{r}_i)\, \mathbf{U}_i, \tag{2.5}$$

where N is the number of particles. The brackets $\langle\ \rangle$ denote the spatial weighted average.

In the obvious fashion, the effective displacement may be defined as

$$\langle \mathbf{r} \rangle (t) = \int_0^t \langle \mathbf{u} \rangle (\xi)\, d\xi. \tag{2.6}$$

Finally, for each particle the Lagrangian deviation from this average position is

$$\Delta \mathbf{r}(t) = \int_0^t [\mathbf{U}(\xi) - \langle \mathbf{u} \rangle (\xi)]\, d\xi. \tag{2.7}$$

The position of the particle may be expressed as

$$\mathbf{r} = \mathbf{r}^0 + \langle \mathbf{r} \rangle + \Delta \mathbf{r}. \tag{2.8}$$

By casting the problem into this form it is possible to use a method of analysis very similar to those described in the literature for the laser–Doppler anemometer (Durrani & Greated 1973; George & Lumley 1973) and for atmospheric radar observation (Rogers & Tripp 1964; Srivastava & Atlas 1974).

It is assumed that the scattering is first-order. That is, any portion of the radiation initially scattered from a particle that is rescattered by another is considered negligible. The total received signal is then the superposition of the contributions from the individual scatterers. From (2.2), the sampled output of the mixer is

$$x_s(t) = \text{const.} \times \left[\sum_{n=-\infty}^{+\infty} \delta(t - n\tau_{rp} - \tau_r) \right] \left[\sum_{i=1}^{N} a_i H(\mathbf{r}_i^0 + \langle \mathbf{r} \rangle + \Delta \mathbf{r}_i) \times \cos [\mathbf{k} \,.\, (\mathbf{r}_i^0 + \langle \mathbf{r} \rangle + \Delta \mathbf{r}_i) + \gamma_i] \right] \tag{2.9}$$

or

$$x_s(t) = \text{const.} \times \left[\sum_{n=-\infty}^{+\infty} \delta(t - n\tau_{rp}) \right] [A^2(t) + B^2(t)]^{\frac{1}{2}} \cos (\mathbf{k} \,.\, \langle \mathbf{r} \rangle + \Phi), \tag{2.10}$$

where

$$A(t) = \sum_{i=1}^{N} a_i H(\mathbf{r}_i^0 + \langle \mathbf{r} \rangle + \Delta \mathbf{r}_i) \cos (\mathbf{k} \,.\, \mathbf{r}_i^0 + \mathbf{k} \,.\, \Delta \mathbf{r}_i + \gamma_i),$$

$$B(t) = -\sum_{i=1}^{N} a_i H(\mathbf{r}_i^0 + \langle \mathbf{r} \rangle + \Delta \mathbf{r}_i) \sin (\mathbf{k} \,.\, \mathbf{r}_i^0 + \mathbf{k} \,.\, \Delta \mathbf{r}_i + \gamma_i), \tag{2.11}$$

$$\Phi = \arctan [B(t)/A(t)]. \tag{2.12}$$

The particle positions are assumed to be random and independent. The quantities $x(t)$, $A(t)$ and $B(t)$ are sums of large numbers of independent, identically distributed random variables, and are therefore approximately Gaussian random processes. The population of the sample volume is typically of the order of 10^6.

By a process similar to FM detection the time derivative of the argument of the

cosine factor in (2.10) can be evaluated. The result is the quantity that has already been referred to as the detected velocity signal, and is seen to be

$$\omega_{\mathrm{d}} = \frac{d}{dt}[\mathbf{k}.\langle \mathbf{r}\rangle + \Phi(t)] = \frac{2\omega_0}{c}\langle u_1\rangle(t) + \dot{\Phi}(t). \tag{2.13}$$

The first term, as expected, is the Doppler shift caused by the spatial weighted average of the instantaneous particle velocities within the sample volume. Except for the spatial average, it is identical with the highly idealized expression in (1.1). For a small sample volume, the appropriately scaled power spectrum of this term gives an estimate of the energy spectrum of the flow velocities.

The quantity ω_{d} also contains a second term: $\dot{\Phi}(t)$. Since $\dot{\Phi}(t)$ is a function of $A(t)$ and $B(t)$, it is a random process. Unfortunately, this partially obscures the detection of the first term that contains the desired quantity: $\langle u_1\rangle$. Clearly, it is important to determine the extent to which this quantity distorts the desired estimate. The nature of $\dot{\Phi}(t)$ is addressed in § 2.3.

2.2. *The Doppler-signal power spectrum*

The spectrum of the Doppler signal is most easily derived by first determining the autocorrelation function and then computing the Fourier transform. Using (2.9), the autocorrelation of the sampled output of the mixer is

$$\begin{aligned} R_{\mathrm{s}}(t, t+\tau) = E\{x_{\mathrm{s}}(t)\, x_{\mathrm{s}}(t+\tau)\} = \text{const.} \times \left[\sum_{n=-\infty}^{+\infty} \delta(\tau - n\tau_{\mathrm{rp}})\right] \\ \times E\left[\sum_{i=1}^{N} a_i H(\mathbf{r}_i^0 + \langle \mathbf{r}\rangle(t) + \Delta\mathbf{r}_i(t)) \cos(\mathbf{k}.(\langle \mathbf{r}\rangle(t) + \Delta\mathbf{r}_i(t)) + \gamma_i)\right] \\ \times \left[\sum_{j=1}^{N} a_j H(\mathbf{r}_j^0 + \langle \mathbf{r}\rangle(t+\tau) + \Delta\mathbf{r}_j(t+\tau)) \cos(\mathbf{k}.(\langle \mathbf{r}\rangle(t) + \Delta\mathbf{r}_j(t+\tau)) + \gamma_j)\right], \end{aligned} \tag{2.14}$$

where the expected value must be taken over the five random quantities, a_i, γ_i, $\mathbf{r}_i^0$, $\langle \mathbf{r}\rangle(t)$ and $\Delta\mathbf{r}_i(t)$.

In evaluating this expression the following assumptions are made.

(i) The particles are independent. That is, the position of one particle does not influence the position of others. This is only precisely true at low volumetric concentrations.

(ii) The particles follow faithfully the motion of the fluid in which they are suspended.

(iii) The representative length of the sample volume is large when compared with the wavelength of the transmitted sound.

(iv) The relative motion of the particle, $\langle \mathbf{r}\rangle + \Delta\mathbf{r}_i$, is independent of the initial position $\mathbf{r}^0$, of the particle.

(v) The scattering amplitude and phase have non-zero, time-invariant mean-squared values.

(vi) The mean velocity gradient within the sample volume is zero. In this instance this should be interpreted to mean that the mean velocity differences within the sample volume are small.

(vii) The probability of finding a particle within a small volume Δv is constant throughout the medium.

A detailed evaluation of (2.14), given these restrictions, is derived by Garbini (1978). The result may be expressed as

$$R_s(\tau) = \text{const.} \times \left[\sum_{n=-\infty}^{+\infty} \delta(\tau - n\tau_{rp})\right] \int_{\text{space}} \cos k_1 z_1 \, Q(\mathbf{z}) P_{\mathbf{z}}(\mathbf{z}, \tau) \, d\mathbf{z}, \tag{2.15}$$

where

$$Q(\zeta) = \int_{-\infty}^{+\infty} H(\xi) \, H(\zeta + \xi) \, d\xi \tag{2.16}$$

is the spatial (three-dimensional) autocorrelation of the sample-volume directivity function. Also

$$\mathbf{z} = [\langle \mathbf{r} \rangle (t+\tau) - \langle \mathbf{r} \rangle (t)] + [\Delta \mathbf{r}(t+\tau) - \Delta \mathbf{r}(t)], \tag{2.17}$$

and $P_{\mathbf{z}}(\mathbf{z}, \tau)$ is the probability-density function of $\mathbf{z}$.

The variable $\mathbf{z}$ is the distance that a particle moved during the time τ. The probability-density function of $\mathbf{z}$ has been described by Batchelor (1949) for turbulent motion assumed to be homogeneous and approximately statistically steady in time as a Gaussian function of the form

$$P_{z_1 z_2 z_3}(z_1, z_2, z_3, \tau) = \frac{1}{(2\pi)^{\frac{3}{2}} |K_{z_{ij}}|^{\frac{1}{2}}} \exp\left[-\tfrac{1}{2}(z_i - \overline{\langle u_i \rangle} \tau) \, K_{z_{ij}}^{-1} (z_j - \overline{\langle u_j \rangle} \tau)\right], \tag{2.18}$$

where $\overline{\langle u_i \rangle}$ is the temporal average of the spatial average of the velocities within the sample volume in the i-direction (the mean velocity in the ith direction for uniform flow). The overbar is used to denote a temporal average.

$$K_{z_{ij}} = E[z_i - \overline{\langle u_j \rangle} \tau) \, (z_j - \overline{\langle u_j \rangle} \tau)] \tag{2.19}$$

is the covariance matrix.

Aside from the summation of delta functions in (2.15), which is the result of the sampling nature of the pulsed ultrasonic velocimeter, this formulation of the autocorrelation function is similar to that described by Edwards & Angus (1971) for the laser–Doppler velocimeter.

In general, the complexity of $P_{\mathbf{z}}(\mathbf{z}, \tau)$ and $Q(\mathbf{z})$ make (2.15) difficult to evaluate. However, for certain cases, useful, closed-form calculations are possible. Consider the case of isotropic turbulence. Here off-diagonal terms in the covariance matrix $K_{z_{ij}}$ are zero. The mean-square values of each of the three diagonal components of $K_{z_{ij}}$ may be expressed as (Batchelor 1949)

$$E[(z - \overline{\langle u \rangle} \tau)^2] = 2\overline{u'^2} \int_0^{\tau} (\tau - \xi) \, R_L(\xi) \, d\xi, \tag{2.20}$$

where $(\overline{u'^2})^{\frac{1}{2}}$ is the turbulence intensity and $R_L(\tau)$ is the Lagrangian time-correlation function. This expression for $E[z - \overline{\langle u \rangle} \tau)^2]$ may be simplified greatly if τ is much smaller than the Lagrangian integral time scale τ_L. For this condition $R_L(\tau) \simeq 1$, and therefore

$$E[(z - \overline{\langle u \rangle} \tau)^2] \simeq \overline{u'^2} \tau^2. \tag{2.21}$$

The autocorrelation function described in (2.15) consists of a decaying sinusoid with its maximum value at $\tau = 0$. The length of time t^* for which the autocorrelation

function is significantly non-zero, may be determined by examining the individual functions within the integral.

First, consider a small sample volume in which the dimension in the direction of the mean flow is small with respect to the Lagrangian integral length scale

$$\Lambda = \tau_{\mathrm{L}}\overline{(u'^2)}^{\frac{1}{2}}. \tag{2.22}$$

The time required for a particle to traverse the sample volume will correspond to the maximum correlation t^*. For a sample volume of width l_t

$$t^* = l_t/\overline{\langle u\rangle}. \tag{2.23}$$

The maximum significant correlation time t^* may be compared with the Lagrangian integral time scale τ_{L}:

$$\frac{t^*}{\tau_{\mathrm{L}}} = \frac{l_t}{\Lambda}\frac{\overline{(u'^2)}^{\frac{1}{2}}}{\overline{\langle u\rangle}}. \tag{2.24}$$

By hypothesis, both of the factors on the right-hand side are small. Therefore, the 'small-time' approximation of (2.21) is valid.

Next, consider a very large sample volume. For purposes of illustration, and with little loss in generality, assume that $Q(z_1, z_2, z_3)$ may be written (in scalar form) as

$$Q(z_1, z_2, z_3) = Q_1(z_1)\,Q_2(z_2)\,Q_3(z_3). \tag{2.25}$$

Then the autocorrelation expression (2.15) may be factored into three terms, each corresponding to a co-ordinate direction. Consider the term associated with the direction of the ultrasonic beam,

$$\int_{-\infty}^{+\infty} \cos k_1 z_1\, Q_1(z_1)\, P_{z_1}(z_1, \tau)\, dz_1. \tag{2.26}$$

If the length of the sample volume is very long in this direction then $Q_1(z_1) = 1$. In practice this might be attained by using a long burst duration. As τ increases, the width of the probability-density function becomes large in comparison with the period of the sinusoidal component. The integral will therefore be very small. That is, the autocorrelation will be significant for times smaller than t^* such that

$$E[(z(t^*) - \overline{\langle u\rangle} t^*)^2] = \left(\frac{2\pi}{k_1}\right)^2 = \tfrac{1}{4}\lambda^2. \tag{2.27}$$

In words, t^* is approximately the time required for a particle to drift one wavelength relative to the mean flow. From (2.27), (2.21) and (2.22), this time t^* is compared with the Lagrangian integral time scale as follows:

$$\frac{t^*}{\tau_{\mathrm{L}}} = \frac{\lambda}{2\overline{(u'^2)}^{\frac{1}{2}}}\frac{\overline{(u'^2)}^{\frac{1}{2}}}{\Lambda} = \frac{\lambda}{2\Lambda}. \tag{2.28}$$

Therefore, for both small and large sample volumes and for flow conditions and wavelengths which satisfy the above conditions, the longest time that need be considered in the autocorrelation function is much smaller than the Lagrangian integral time scale.

Throughout the remainder of this discussion it will be assumed that $t^*/\tau_L \ll 1$, according to (2.24) or (2.28), and therefore the small-time approximation of (2.21) is valid.

The effective directivity of the sample volume of the pulsed ultrasonic Doppler velocimeter is a complicated function of the pulse shape, the transducer damping characteristics, the shape of the focused beam, the receiver and subsequent detection circuits. In general, this function is three-dimensional and continuous, with maximum value at the centre and decreasing nearly monotonically towards the edges. Several approximations for the directivity function can be found in the literature (Newhouse 1973; Jorgensen & Garbini 1974), but the assumption of a Gaussian-shaped directivity function has particular mathematical and heuristic advantages in this case. That is,

$$H(r_1, r_2, r_3) = \frac{1}{(2\pi)^{\frac{3}{2}}\sigma_1\sigma_2\sigma_3} \exp\left\{-\frac{1}{2}\left[\left(\frac{r_1}{\sigma_1}\right)^2 + \left(\frac{r_2}{\sigma_2}\right)^2 + \left(\frac{r_3}{\sigma_3}\right)^2\right]\right\}. \tag{2.29}$$

where σ_1, σ_2, σ_3 represent the widths of the sample volume along the major axes. It will be seen later that such an assumption compares favourably with measurements of the distribution function of highly focused transducers. It follows that the three-dimensional autocorrelation function of (2.16) may be expressed as

$$Q(r_1, r_2, r_3) = \frac{1}{8\pi^{\frac{3}{2}}\sigma_1\sigma_2\sigma_3} \exp\left\{-\frac{1}{4}\left[\left(\frac{r_1}{\sigma_1}\right)^2 + \left(\frac{r_2}{\sigma_2}\right)^2 + \left(\frac{r_3}{\sigma_3}\right)^2\right]\right\}. \tag{2.30}$$

The autocorrelation function for the laser–Doppler anemometer, for one dimension, having a Gaussian-shaped sample volume, may be found in the literature (George & Lumley 1973). On applying (2.15) for the pulsed ultrasonic Doppler velocimeter this result may be extended in a straightforward fashion to three dimensions. The autocorrelation function is seen to be

$$\begin{aligned} R_s(\tau) = \text{const.} \times &\left[\sum_{n=-\infty}^{+\infty} \delta(t - n\tau_{rp})\right]\left[\prod_{i=1}^{3}\left(1 + \frac{\overline{u_i'^2}\tau^2}{2\sigma_i^2}\right)\right]^{-\frac{1}{2}} \\ &\times \exp\left\{-\frac{1}{4}\left[\sum_{i=1}^{3} \frac{\overline{\langle u_i\rangle^2}\tau^2}{\sigma_2^2\left(1 + \frac{\overline{u_i'^2}\tau^2}{2\sigma_i^2}\right)}\right]\right\} \exp\left\{-\frac{1}{2}\left[\frac{\overline{k^2u_1'^2}\tau^2}{1 + \frac{\overline{u_1'^2}\tau^2}{2\sigma_1^2}}\right]\right\} \\ &\times \cos\left[\frac{\overline{k\langle u_1\rangle}\tau}{1 + \frac{\overline{u_1'^2}\tau^2}{2\sigma_1^2}}\right]. \end{aligned} \tag{2.31}$$

For the small-sample-volume case, from (2.23) and (2.24),

$$\tau^2 \ll \frac{\sigma_1^2}{\overline{\langle u_1\rangle^2}}, \tag{2.32}$$

and $(\overline{u_1'^2})^{\frac{1}{2}}/\overline{\langle u_1\rangle}$ is small by assumption, therefore

$$\frac{\overline{u_1'^2}\tau^2}{2\sigma_1^2} = \frac{1}{2}\frac{\overline{\langle u_1\rangle^2}\tau^2}{\sigma_1^2}\frac{\overline{u_1'^2}}{\overline{\langle u_1\rangle^2}} \ll 1. \tag{2.33}$$

Also, for the case of a large sample volume, from (2.28),

$$\tau^2 \ll \left(\frac{2\pi}{k(\overline{u'^2})^{\frac{1}{2}}}\right)^2 = \left(\frac{\lambda}{(\overline{u'^2})^{\frac{1}{2}}}\right)^2 \tag{2.34}$$

and, since λ/σ_1 is small by assumption, therefore

$$\frac{\overline{u'^2}\tau^2}{2\sigma_1^2} = \frac{1}{2}\left(\frac{\overline{u'^2}\tau^2}{\lambda^2}\right)\left(\frac{\lambda^2}{\sigma_1^2}\right) \ll 1. \tag{2.35}$$

Therefore the expression for the autocorrelation may be rewritten in considerably simpler form as

$$R_s(\tau) = \text{const.} \times \left[\sum_{n=-\infty}^{+\infty} \delta(\tau - n\tau_{rp})\right] \exp\left\{-\left[\tfrac{1}{2}\overline{\Delta u_1'^2}\tau^2 k^2 + \tfrac{1}{4}\tau^2\left(\frac{\overline{\langle u_1\rangle^2}}{\sigma_1^2} + \frac{\overline{\langle u_2\rangle^2}}{\sigma_2^2} + \frac{\overline{\langle u_3\rangle^2}}{\sigma_3^2}\right)\right]\right\} \exp - \left[\frac{k^2\overline{\langle u_1\rangle'^2}\tau^2}{2}\right] \cos k\overline{\langle u_1\rangle}\tau, \tag{2.36}$$

where $\overline{\langle u_1\rangle'^2}$ is the variance of the spatially averaged velocity fluctuations in the e_1-direction and $\overline{\Delta u_1'^2}$ is the variance of the deviation of the velocities within the sample volume from the spatially averaged velocity. It may be shown that

$$\overline{\Delta u'^2} = \overline{u'^2} - \overline{\langle u\rangle'^2}. \tag{2.37}$$

The power spectrum of the sampled output of the mixer is obtained by taking the Fourier transform of the autocorrelation (2.36). Applying the Fourier convolution theorem, we have

$$S_s(\omega) = \text{const.} \times \sum_{n=-\infty}^{+\infty} \left[\exp \frac{\left(\omega - k\overline{\langle u_1\rangle} - \frac{2\pi n}{\tau_{rp}}\right)^2}{2\Delta\omega_c^2} + \exp \frac{\left(\omega + k\overline{\langle u_1\rangle} - \frac{2\pi n}{\tau_{rp}}\right)^2}{2\Delta\omega_c^2}\right], \tag{2.38}$$

where

$$\Delta\omega_c^2 = k^2\overline{\Delta u_1'^2} + \frac{1}{2}\left(\frac{\overline{\langle u_1\rangle^2}}{\sigma_1^2} + \frac{\overline{\langle u_2\rangle^2}}{\sigma_2^2} + \frac{\overline{\langle u_3\rangle^2}}{\sigma_3^2}\right) + k^2\overline{\langle u_1\rangle'^2}. \tag{2.39}$$

Finally, the Doppler signal is produced by applying the sampled output of the mixer to a 'hold' circuit where the value of each sample is sustained continuously until the next sample. The result is low-pass filtered to remove high-frequency harmonics of the 'hold' pulses. The Doppler spectrum is

$$S_{SH}(\omega) = S_s(\omega)\left[\tau_{rp}\frac{\sin(\frac{1}{2}\omega\tau_{rp})}{\frac{1}{2}\omega\tau_{rp}}\right]^2 |F(\omega)|^2, \tag{2.40}$$

where $|F(\omega)|^2$ is the square of the magnitude of the low-pass filter function.

If the filter is considered to be ideal, and of such width that only the first term in the summation in (2.38) is retained, then the spectrum becomes

$$S_{SH}(\omega) = \text{const.} \times \left[\exp - \frac{(\omega - k\overline{\langle u_1\rangle})^2}{2\Delta\omega_c^2} + \exp - \frac{(\omega + k\overline{\langle u_1\rangle})^2}{2\Delta\omega_c^2}\right]\left[\tau_{rp}\frac{\sin\frac{1}{2}\omega\tau_{rp}}{\frac{1}{2}\omega\tau_{rp}}\right]^2. \tag{2.41}$$

Also, if the pulse-repetition frequency is much higher than the highest significant frequency component in the first factor in (2.41), then

$$S_{SH}(\omega) = \left[\exp - \frac{(\omega - k\overline{\langle u_1\rangle})^2}{2\Delta\omega_c^2} + \exp - \frac{(\omega + k\overline{\langle u_1\rangle})^2}{2\Delta\omega_c^2}\right], \tag{2.42}$$

where the result has been normalized with respect to the total power. From this expression and that of (2.39), it is seen that the Doppler-signal spectrum is centred at the

frequency corresponding to the spatial-average velocity in the beam direction and is approximately Gaussian in shape. The width of the spectrum, $\Delta\omega_c$ in (2.39), may be related to the standard deviation of the turbulent-velocity fluctuations and to the time required for a particle to traverse the sample volume in the direction of the mean flow (transit-time effect). In general, other effects can also be sources of broadening in the Doppler-signal spectrum. These may include: (i) gradients in mean velocity within the sample volume; (ii) geometric effects resulting from large sample volumes in the near field of unfocused transducers (Newhouse, Varner & Bendick 1977); (iii) deviation from idealized signal processing; or (iv) anisotropic or non-stationary turbulence effects. For the situations considered here these factors are small and will be neglected.

The intensity of the turbulence velocity fluctuations is defined as the ratio of r.m.s. velocity fluctuations to the local mean velocity. Equations (2.2), (2.37), (2.39) and (2.42) indicate that the turbulence intensity may be evaluated from measurements of the mean and width of the Doppler-signal spectrum according to

$$\text{intensity} = \left[\left(\frac{\Delta\omega_c}{\bar{\omega}}\right)^2 \cos^2\theta - \alpha^2\right]^{\frac{1}{2}}, \tag{2.43}$$

where $\Delta\omega_c$ and $\bar{\omega}$ are respectively the width and mean of the Doppler-signal spectrum, and α is a parameter descriptive of the velocimeter:

$$\alpha = \frac{\lambda}{4\sqrt{2\,\pi\sigma_v}}, \tag{2.44}$$

where σ_v is the width of the sample volume in the direction of the mean flow, λ is the wavelength of the acoustic carrier and θ is the Doppler angle. An interesting situation arises when the sample volume can be made sufficiently large with respect to the wavelength such that the second term in (2.43) is very small. In that case, $\Delta\omega_c/\bar{\omega}$ may be interpreted directly as a measure of the turbulence intensity without any knowledge of the velocimeter parameters σ_v and λ. For the usual ranges of permissible wavelengths and intensities, this condition could only exist for very *large* sample volumes.

2.3. *The Doppler-ambiguity power spectrum*

An estimate of the one-dimensional energy spectrum for the direction parallel to the ultrasonic beam may be obtained by computing the power spectrum of the detected velocity signal. From (2.13), this signal is equal to

$$\omega_d = \frac{d}{dt}[(\mathbf{k}\,.\,\langle\mathbf{r}\rangle) + \Phi(t)]. \tag{2.45}$$

The first term is the instantaneous spatial average of the velocity components in the direction of the ultrasonic beam, as in (2.5). The second term is an unwanted artifact arising from the measurement process. In the analysis of both radar systems and laser–Doppler velocimeters the quantity analogous to this term is referred to as the Doppler ambiguity. The contribution of this quantity to the Doppler velocity signal is very important to the measurement of the one-dimensional spectrum.

Since it may be shown that $\langle\mathbf{r}\rangle$ and Φ are independent, the spectral process of the sum of the two terms in (2.45) is equal to the sum of the spectral processes. That is,

$$S_{\omega_d}(\omega) = S_{\langle u_1\rangle}(\omega) + S_{\dot{\Phi}}(\omega). \tag{2.46}$$

The relationship between the spectrum of the spatial average of the velocity, $S_{\langle u_1\rangle}(\omega)$ and the true one-dimensional spectrum is discussed in § 2.4.

Determination of the spectrum of the Doppler-ambiguity term $S_{\dot\Phi}(\omega)$, where $\dot\Phi$ is described in (2.12), and $A(t)$ and $B(t)$ are Gaussian, is a classical problem of FM signal-detection theory. It was first examined by Rice (1945, 1949) and more generally formalized by Middleton (1950) and Lawson & Ulenbech (1950). The correlation function of $\dot\Phi$ is

$$R_{\dot\Phi}(\tau) = E(\dot\Phi(t)\,\dot\Phi(t+\tau)] = \left[\frac{\dot g^2(\tau) - g(\tau)\,\ddot g(\tau)}{2g^2(\tau)}\right]\ln(1-g^2(\tau)), \tag{2.47}$$

where

$$g(\tau) = \frac{R_A(\tau)}{R_A(0)} = \frac{E[A(t)\,A(t+\tau)]}{E[A^2]} = \frac{E[B(t)\,B(t+\tau)]}{E[B^2]}. \tag{2.48}$$

In general, the correlation coefficient $g(\tau)$, and therefore $R_{\dot\Phi}(\tau)$, are functions of the sample-volume specification. From (2.47) and (2.48), as τ approaches zero, the value of the autocorrelation becomes logarithmically infinite. This indicates that the mean-square value of the PUDV velocity signal will be infinite. Of course, in practice the bandwidth of $\omega_{\rm d}$ is limited so that the actual signal has finite power. However, this does demonstrate that attempting to equate the r.m.s. value of the detected velocity signal to the r.m.s. value of the actual velocity fluctuations is likely to result in substantial errors.

An expression for the autocorrelation of $A(t)$ has been computed in Garbini (1978). The calculation is similar to that of the correlation function of the Doppler signal, except that the expectations are taken over α_i, γ_i, $\mathbf{r}_i^0$, $\langle\mathbf{r}\rangle$, and $\Delta\mathbf{r}_i$.

For the case of a general sample volume described in terms of $Q(r_1, r_2, r_3)$ defined by (2.16), and using (2.11) and (2.48), the correlation coefficient is

$$g(\tau) = \int_{-\infty}^{+\infty} \cos k\delta_1 \int_{-\infty}^{+\infty} Q(\mathbf{R}+\boldsymbol{\delta})\,P_{\mathbf{R}}(\mathbf{R},\tau)\,d\mathbf{R}\,P_{\boldsymbol{\delta}}(\boldsymbol{\delta},\tau)\,d\boldsymbol{\delta}, \tag{2.49}$$

where

$$\mathbf{R} = \langle\mathbf{r}\rangle(t+\tau) - \langle\mathbf{r}\rangle(t), \quad \boldsymbol{\delta} = \Delta\mathbf{r}(t+\tau) - \Delta\mathbf{r}(t), \tag{2.50}$$

and $P_{\mathbf{R}}(\mathbf{R},\tau)$ and $P_{\boldsymbol{\delta}}(\boldsymbol{\delta},\tau)$ are the respective probability functions.

Again, it is assumed that (i) the turbulence is homogeneous, and that there are no mean velocity gradients, and that (ii) the 'small-time' approximation for particle motion is valid. Then

$$\begin{gathered} E[R_i] = \overline{\langle u_i\rangle}\,\tau, \quad E[\delta_i] = 0, \\ E[(R_i - \overline{\langle u_i\rangle}\,\tau)^2] = \overline{\langle u\rangle'^2}\,\tau^2, \quad E[\delta_i^2] = \overline{(u'^2 - \overline{\langle u_i\rangle'^2})}\,\tau^2 = \overline{\Delta u'^2}\tau^2; \end{gathered} \tag{2.51}$$

and the probability density functions are of the form

$$P_{R_1R_2R_3}(R_1,R_2,R_3,\tau) = \frac{1}{(2\pi)^{\frac{3}{2}}\,|K_R|^{\frac{1}{2}}} \exp\left[-\tfrac{1}{2}(R_i - \overline{\langle u_i\rangle}\,\tau)\,K_{Rij}^{-1}(R_j - \overline{\langle u_j\rangle}\,\tau)\right], \tag{2.52}$$

$$P_{\delta_1\delta_2\delta_3}(\delta_1,\delta_2,\delta_3,\tau) = \frac{1}{(2\pi)^{\frac{3}{2}}\,|K_{\delta ij}|^{\frac{1}{2}}} \exp\left[-\tfrac{1}{2}\delta_i K_{\delta ij}^{-1}\delta_j\right]. \tag{2.53}$$

If, as in § 2.2, we examine the specific case of a Gaussian-shaped sample-volume distribution function of the form given in (2.29), the form of the correlation coefficient is

$$g(\tau) = \exp\left[-\tfrac{1}{2}\Delta^2\tau^2\right], \tag{2.54}$$

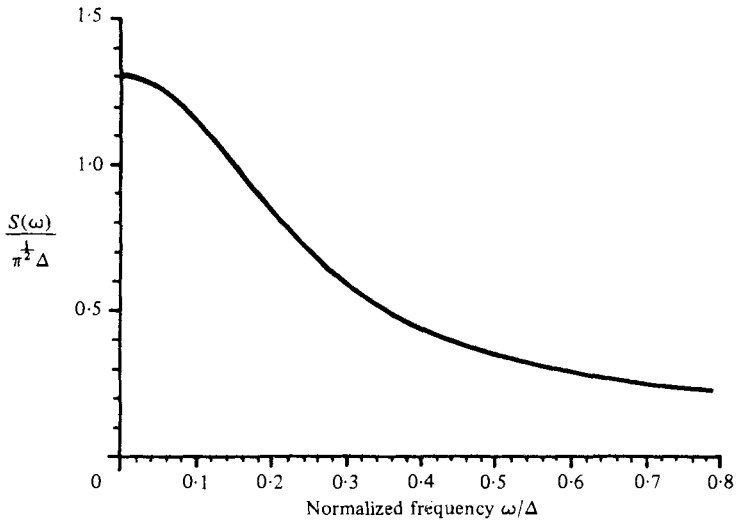

FIGURE 3. Power spectrum of the Doppler-ambiguity process.

where

$$\Delta^2 = \frac{1}{2}\left(\frac{\overline{\langle u_1\rangle^2}}{\sigma_1^2} + \frac{\overline{\langle u_2\rangle^2}}{\sigma_2^2} + \frac{\overline{\langle u_3\rangle^2}}{\sigma_3^2}\right) + k^2\overline{\Delta u_1'^2}. \tag{2.55}$$

The spectrum, corresponding to the Fourier transform of (2.47), when $g(\tau)$ is of the form indicated by (2.54), was determined by Rice (1949). Applied to this specific case it is

$$S_\Phi(\omega) = \tfrac{1}{2}\pi^{\frac{1}{2}}\Delta \sum_{n=1}^{\infty} n^{-\frac{3}{2}} \exp\left[-\frac{\omega^2}{4n\Delta^2}\right]. \tag{2.56}$$

Similar expressions exist for the one-dimensional case of the laser–Doppler velocimeter (Durrani & Greated 1973; George & Lumley 1973). The function S_Φ is plotted in figure 3. Notice that the magnitude of the ambiguity spectrum at the origin is directly proportional to the quantity Δ. The two terms in Δ^2, from (2.55), can be identified as the primary causes of ambiguity noise. The first term in Δ^2 corresponds to the square of the inverse of the transit time through the sample volume. A decrease in the transit time will therefore cause an increase in the level of the ambiguity spectrum.

The second term is associated with the mean-square deviations of individual particle velocities from the spatial average of the velocity. Therefore an increase in the turbulence itself will contribute to an increase in the ambiguity level.

Figure 4 illustrates the large extent to which the ambiguity spectrum corrupts the estimate of the one-dimensional energy spectrum. Shown are the one-dimensional energy spectrum for flow in a pipe (Laufer 1954), and a theoretical prediction of the same quantity as measured with high-resolution pulsed ultrasonic Doppler velocimeter under typical conditions (major sample-volume dimension = 1 mm).

The ambiguity level for a typical laser velocimeter is also indicated for purposes of comparison. For the normalization shown in this figure, the level of the ambiguity component of the spectrum as k approaches zero is proportional to the square of the instrument carrier wavelength. The laser device will nearly always have a substantially lower ambiguity level. The principal reason for this advantage is the lower corresponding value of wavelength obtainable.

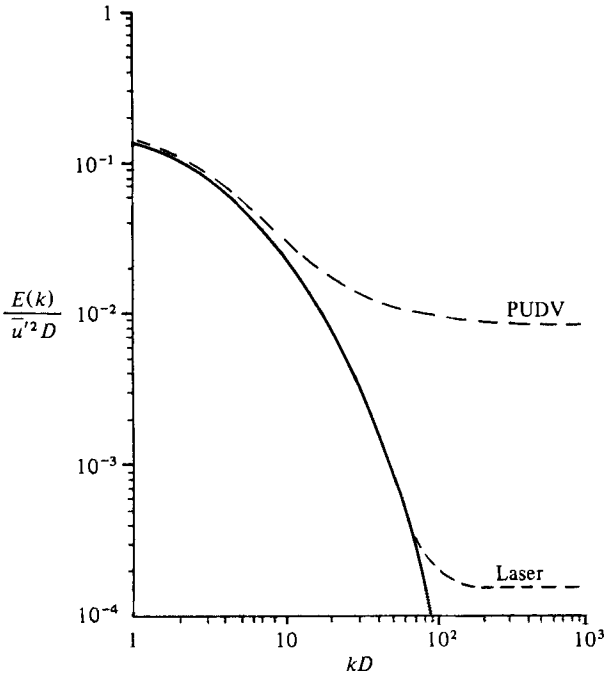

FIGURE 4. Spectrum of the velocity fluctuations for pipe flow, as measured with pulsed ultrasonic and the laser velocimeters. $U = 54$ cm/s, $D = 2{\cdot}54$ cm.

For the ultrasonic measurement, the large Doppler ambiguity imposes a severe restriction on the value of the velocity spectral estimate. Traditional parameters of turbulence, such as intensity, microscale and integral scale, are usually computed from measurements of the turbulence spectrum or deduced directly from the time history of the velocity. Unless the magnitude of the Doppler-ambiguity components can be reduced relative to those associated with velocity fluctuations, calculations of this type are meaningless.

From (2.13), (2.46) and (2.56), the value of the velocity components can be raised in proportion to that of the ambiguity process by increasing the acoustic carrier frequency. However, such an increase is not always practical. Attenuation of acoustic energy usually increases rapidly with frequency. Therefore a high-frequency carrier can limit the useful range of the instrument.

Another method of reducing the ambiguity component $S_{\dot{\Phi}}(\omega)$ is to increase the transit time by increasing the size of the sample volume. This also has limited advantages. Section 2.4 illustrates that the dimensions of the sample volume must not be made arbitrarily large.

Examples of the effects of the Doppler ambiguity on turbulent measurements are examined much more intensively in the experimental portion of this study (Garbini *et al.* 1982).

2.4. *Attenuation of spectra due to finite sample volume*

Because the sample volume is of finite size, the measured velocity represents a spatial average of the velocity weighed by the effective sample volume directivity function rather than the velocity at a particular point. This causes partial attenuation of even

large velocity fluctuations and virtual insensitivity to small eddies. Estimates of turbulence spectra based on these measurements will, therefore, be characterized by progressively greater attenuation at higher frequencies. This problem has been studied extensively in the field of meteorological observations using pulsed radar (Rogers & Tripp 1964; Srivastava & Atlas 1974; Sychra 1972). It is not difficult to show that the basic results can be applied to the pulsed ultrasonic Doppler velocimeter in a straightforward fashion.

Consider the correlation of the velocity signals from two sample volumes, at points α and β, separated in a field of homogeneous turbulence at a distance (r_1, r_2, r_3). Since the ultrasonic velocimeter measures only the velocity components in the direction of the beam (referred to as the 1-direction), denote the correlation of the spatial-averaged velocities as

$$\overline{\langle u_1\rangle_\alpha \langle u_1\rangle_\beta} = \langle P_{11}(r_1, r_2, r_3)\rangle. \tag{2.57}$$

Here, the brackets $\langle\ \rangle$ refer to the quantities computed from the spatially averaged velocities. Then, from (2.5) and (2.57),

$$\langle P_{11}(r_1, r_2, r_3)\rangle = \int\int\int_{-\infty}^{+\infty} P_{11}(\gamma_1, \gamma_2, \gamma_3)\, Q(\gamma_1 + r_1, \gamma_2 + r_2, \gamma_3 + r_3)\, d\gamma_1 d\gamma_2 d\gamma_3, \tag{2.58}$$

where $P_{11}(r_1, r_2, r_3) = \overline{(u_1)_\alpha (u_1)_\beta}$ is the correlation function for the true velocities in the 1-direction at points α and β. The function $Q(r_1, r_2, r_3)$, originally defined in (2.16), is the three-dimensional autocorrelation function of the effective sample volume directivity.

Taking the Fourier transform of (2.58), the (1, 1)-component of the three-dimensional spatially averaged spectrum tensor is

$$\langle E_{11}(k_1, k_2, k_3)\rangle = E_{11}(k_1, k_2, k_3)\, \mathscr{F}_3 Q(k_1, k_2, k_3), \tag{2.59}$$

where $E_{11}(k_1, k_2, k_3)$ is the (1, 1)-component of the actual three-dimensional spectrum tensor, and $\mathscr{F}_3 Q(k_1, k_2, k_3)$ is the three-dimensional Fourier transform of $Q(r_1, r_2, r_3)$. The quantities (k_1, k_2, k_3) are the components of the wavenumber vector. In words, the measured spectrum is equal to the actual spectrum filtered in three dimensions by Q.

The relationship between the three-dimensional and the one-dimensional longitudinal spectra is given by

$$\langle E_{\mathrm{L}}(k_1)\rangle = \int\int_{-\infty}^{+\infty} \langle E_{11}(k_1, k_2, k_3)\rangle\, dk_2 dk_3, \tag{2.60}$$

and the corresponding correlation is related by the Fourier transform,

$$\langle P_{11}(r_1, 0, 0)\rangle = \frac{1}{2}\int_{-\infty}^{+\infty} \langle E_{\mathrm{L}}(k_1)\rangle\, e^{ik_1 r_1} dk_1. \tag{2.61}$$

For isotropic turbulence, the relationship between the spatial-average one-dimensional transverse spectrum and corresponding correlation function is given by

$$\langle E_{\mathrm{T}}(k_2)\rangle = \int_{-\infty}^{+\infty} \langle E_{11}(k_1, k_2, k_3)\rangle\, dk_1 dk_3, \tag{2.62}$$

$$\langle P_{11}(0, r_2, 0)\rangle = \frac{1}{2}\int_{-\infty}^{+\infty} \langle E_{\mathrm{T}}(k_2)\rangle\, e^{ik_2 r_2} dk_2. \tag{2.63}$$

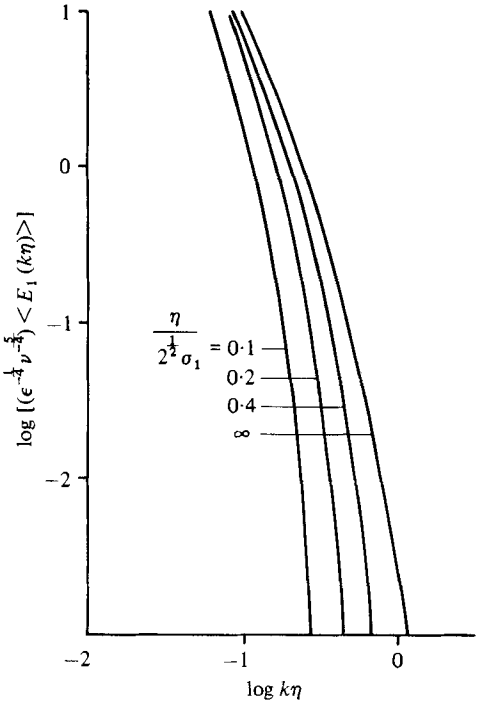

FIGURE 5. Attenuation of the one-dimensional turbulence spectrum due to finite sample-volume size.

The mean-square value of the spatially averaged velocity fluctuations, referred to in previous sections, is

$$\overline{\langle u\rangle'^2} = \int_{-\infty}^{+\infty} \langle E_{\mathrm{L}}(k_1)\rangle\, dk_1 = \int_{-\infty}^{+\infty} \langle E_{\mathrm{L}}(k_2)\rangle\, dk_2. \tag{2.64}$$

To illustrate the effects of spatial attenuations, it is useful to examine the specific case of a Gaussian-shaped sample-volume directivity function and isotropic incompressible flow. For these circumstances the vector velocity field is solenoidal (zero divergence). If the directivity function is defined by (2.29), theory developed for circular-beam pulsed radar (Sychra 1972) can be adapted to give the measured one-dimensional longitudinal and transverse spectra

$$\langle E_{\mathrm{L}}(k_1)\rangle = \exp[-k_1^2\sigma_1^2]\int_{k_1}^{\infty} \exp[-\sigma_2^2(\xi^2-k_1^2)]\frac{\xi^2-k_1^2}{\xi^3}E(\xi)\,d\xi, \tag{2.65}$$

$$\langle E_{\mathrm{T}}(k_2) = \exp[-k_2^2\sigma_2^2]\int_{k_2}^{\infty} \Psi[(\xi^2-k_2^2)^{\frac{1}{2}}]\frac{E(\xi)}{2\pi\xi^3}d\xi, \tag{2.66}$$

where

$$\Psi(\rho) = 2\int_0^{\pi} \exp[-\rho^2(\sigma_1^2\cos^2\theta+\sigma_2^2\sin^2\theta)]\,[k_2^2+\rho^2\sin^2\theta]\,d\theta, \tag{2.67}$$

$E(k)$ is the three-dimensional energy-spectrum function, and σ_1 and σ_2 are respectively the axial and cross-beam dimensions of the sample volume.

For purposes of demonstration assume that the sample volume is spherical ($\sigma_1 = \sigma_2$) and that $E(k)$ is of the form described by Pao (1965) for the small-scale structure of turbulence at very large wave and Reynolds numbers:

$$E(k) = \alpha \epsilon^{\frac{2}{3}} k^{-\frac{5}{3}} \exp\left(-\tfrac{3}{2}\alpha \nu \epsilon^{-\frac{1}{3}} k^{\frac{4}{3}}\right), \quad \alpha = 1{\cdot}7, \tag{2.68}$$

where ϵ is the dissipation per unit mass and ν is the kinematic viscosity. Since this form of $E(k)$ has been used in the literature to explore theoretically the spatial attenuation in atmospheric radar and laser velocimeter systems, it may serve as a useful basis for comparison.

The unattenuated longitudinal one-dimensional spectrum and the corresponding spatial-average quantity for various sizes of sample volumes with circular symmetry are shown in figure 5. As an example consider a sample volume for which $\sigma = 0{\cdot}05$ cm, measuring flow with $\epsilon = 27$ cm/s (corresponding to pipe flow, $\bar{U} = 54$ cm/s and $D = 2{\cdot}54$) (Berman & Dunning 1973) which results in $\eta/2^{\frac{1}{2}}\sigma_1 = 0{\cdot}2$. It is clear that the amount of attenuation suffered by the pulsed Doppler velocimeter may be substantial. Sample-volume size in relation to the geometry of the flow will be a major consideration in evaluating the accuracy of the spectral estimate.

In the experimental portion of this investigation it is necessary to predict the amount of spectral attenuation based on thermal-anemometer measurements of actual one-dimensional longitudinal spectra. With the previous assumptions of isotropic turbulence and incompressible flow, the vector velocity field is solenoidal (zero divergence). For that case the three-dimensional energy spectrum $E(k)$ is related to the longitudinal one-dimensional spectrum by

$$E(k) = \tfrac{1}{2}k^3 \frac{d}{dk}\left[\frac{1}{k}\frac{d}{dk}(E_{\mathrm{L}}(k))\right]. \tag{2.69}$$

The second derivative makes direct numerical application of (2.69) to measured data impractical. However, substituting (2.69) into (2.65) and integrating twice by parts yields a form suitable for numerical evaluation. The expression for the spatial average longitudinal spectrum becomes

$$\langle E_{\mathrm{L}}(k_1)\rangle = \exp\left(-\sigma_1^2 k_1^2\right) E_{\mathrm{L}}(k_1) + 2\sigma_2^4 \exp\left[-k_1^2(\sigma_1^2 - \sigma_2^2)\right] \times \int_{k_1}^{\infty} \exp\left(-\sigma_2^2 \xi^2\right)(\xi^2 - k_1^2 - 2/\sigma_2^2)\, E_{\mathrm{L}}(\xi)\, d\xi. \tag{2.70}$$

In compressible flow the resulting vector velocity field is solenoidal, and therefore

$$\sum_{i=1}^{3} \frac{d}{dr_i} P_{1i}(r_1, r_2, r_3) = 0. \tag{2.71}$$

From this expression and the assumption that the field is isotropic, the longitudinal and transverse spectra are related by

$$E_{\mathrm{T}}(k_1) = \frac{1}{2}\left[E_{\mathrm{L}}(k_1) - k_1 \frac{dE_{\mathrm{L}}(k)}{dk_1}\right]. \tag{2.72}$$

However, for an arbitrary sample-volume specification the corresponding relation does not hold for the spectra of the spatial average of the velocity. In fact,

$$\sum_{i=1}^{3} \frac{d}{dr_i} \langle P_{1i}(r_1, r_2, r_3)\rangle = 0 \tag{2.73}$$

is *only* true in the case of a spherically symmetric sample volume ($\sigma_1 = \sigma_2 = \sigma_3$). The correct general expression must be derived directly from (2.66) and (2.69). Again, on integrating twice by parts, the measured transverse spectrum is

$$\langle E_T(k_2)\rangle = -\tfrac{1}{2}\exp(-\sigma_2^2 k_2^2)\left\{k_2\frac{d}{dk_2}[E_L(k_2)] + E_L(k_2)[k_2^2(\sigma_1^2+\sigma_2^2)-1] - \frac{2}{\pi}\int_{k_2}^{\infty} F[(\xi^2-k_2^2)^{\frac{1}{2}}]\,E_L(\xi)\,\xi\,d\xi\right\}, \quad (2.74)$$

where

$$F(\rho) = 2\int_0^{\pi} e^{-\rho^2\gamma}[\gamma(\gamma k^2 - 2\sin^2\theta) + \rho^2\gamma^2\sin^2\theta]\,d\theta, \quad (2.75)$$

$$\gamma = \sigma_1^2\cos^2\theta + \sigma_2^2\sin^2\theta. \quad (2.76)$$

Although this equation requires two-dimensional integration, when carefully programmed it is feasible to evaluate it numerically.

It has been suggested (Sychra 1972) that the spatial-average spectrum for pulsed radar systems might be 'defiltered' to correct the attenuation on the basis of known sample-volume intensity distribution. While this technique has not been extensively employed in those systems, it may become a practical necessity for evaluation of small-scale flows with the pulsed ultrasonic Doppler velocimeter.

At this point it is important that a practical aspect of the measurement of turbulence with the pulsed Doppler velocimeter be discussed. Taylor's hypothesis states that, if the velocity fluctuations are small in comparison with the mean velocity, then the turbulence field may be thought of as being 'frozen' as it is moved past an observation point. The spatial correlation of velocities at two points α and β aligned with the mean velocity direction and separated by r will be approximately equivalent to the time correlation of the velocity at a single point. That is

$$\overline{u_\alpha(t)\,u_\beta(t)} = \overline{u_\alpha(t)\,u_\alpha(t+\tau)}, \quad (2.77)$$

where $\tau = r/\bar{u}$. A typical procedure for evaluating the spatial correlation would be to compute the temporal autocorrelation of the detected velocity signal and then rely on Taylor's hypothesis to relate it to the spatial correlation function.

Correspondingly, the spatial spectrum is expressed in terms of the temporal spectrum by

$$E_1(k_1) = \frac{\overline{U}_1}{\pi}S(\omega), \quad (2.78)$$

where $\overline{U}_1$ is the mean velocity, and Taylor's hypothesis relates the spatial and temporal frequencies by $k_1 = \omega/\overline{U}_1$. Here, $S(\omega)$ is the two-sided (ω: $[-\infty, +\infty]$) velocity spectrum related to the autocorrelation through the Fourier transform. Since the Fourier transform may be defined in several different ways the form used in this analysis is stated at this point for clarity:

$$S(\omega) = \int_{-\infty}^{+\infty} R(\tau)\,e^{-i\omega\tau}\,d\tau, \quad R(\tau) = \frac{1}{2\pi}\int_{-\infty}^{+\infty} S(\omega)\,e^{i\omega\tau}\,d\omega. \quad (2.79)$$

In practice, the ultrasonic beam and the direction of the mean velocity are not often collinear. In this case, the spatial correlation implied under Taylor's hypothesis does

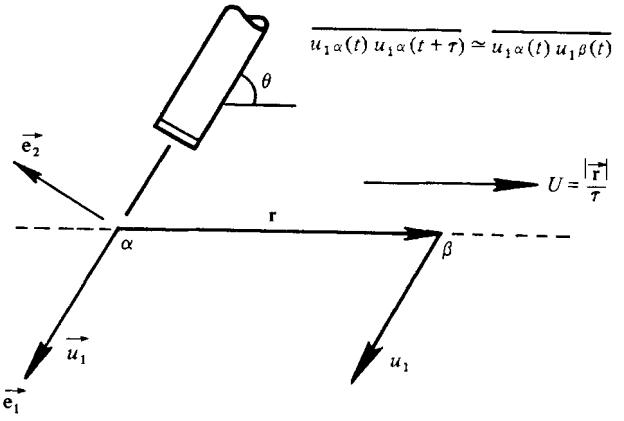

FIGURE 6. Measurement of the correlation function with Doppler angle equal to θ.

not correspond to $\langle P_{11}(r_1, 0, 0)\rangle$ discussed above. Rather, the autocorrelation of the detected velocity signal represents the spatial correlation of the velocity components in the *direction of the beam* as a function of the spatial separation in the *direction of the mean velocity*. This situation is illustrated in figure 6, where θ is the Doppler angle. The correlation corresponds to $\langle P_{11}(r\cos\theta, r\sin\theta, 0)\rangle$. The correlations $\langle P_{11}(r, 0, 0)\rangle$ and $\langle P_{11}(r\cos\theta, r\sin\theta, 0)\rangle$ are distinct even in isotropic turbulence.

Assuming that P_{11} is an element of an isotropic tensor, the skewed correlation is related to the longitudinal and transverse correlations by

$$P_{ij}(r_1, r_2, r_3) = \frac{1}{r^2}[P_{11}(r, 0, 0) - P_{11}(0, r, 0)]\, r_i r_j + P_{11}(0, r, 0)\,\delta_{ij}. \tag{2.80}$$

Therefore it is straightforward to show that, for the situation depicted in figure 6, the measured correlation function corresponds to

$$\langle P_{11}(r\cos\theta, r\sin\theta, 0)\rangle = \langle P_{11}(r, 0, 0)\rangle\cos^2\theta + \langle P_{11}(0, r, 0)\rangle\sin^2\theta. \tag{2.81}$$

Similarly, it follows that the spatial-average spectrum, as measured by the pulsed Doppler velocimeter with Doppler angle equal to θ, can be expressed as

$$\langle E_\theta(k_1)\rangle = \langle E_{\mathrm{L}}(k_1)\rangle\cos^2\theta + \langle E_{\mathrm{T}}(k_1)\rangle\sin^2\theta. \tag{2.82}$$

Therefore (2.70), (2.74) and (2.82) may be used to predict the first term in (2.46) for the spectrum of the detected velocity signal from the actual longitudinal one-dimensional energy spectrum.

3. Ambiguity reduction using two sample volumes

As seen in § 2.3, the Doppler ambiguity is a major source of error in estimating the one-dimensional energy spectrum. One possible method of improving the measurement (investigated by George & Lumley (1973) for the laser–Doppler velocimeter) is to subtract the statistically independent ambiguity spectrum from the measured spectrum. Although a similar procedure might be applied to the pulsed ultrasonic Doppler velocimeter, a disadvantage of this method is that it entails an explicit theoretical prediction of the ambiguity spectrum. This, in turn, requires that the

flow situation correspond precisely to a case for which theoretical results can be practically evaluated and that certain flow-related parameters be known *a priori*. In addition, the ambiguity components of the measured spectrum must be accurately estimated. The improvement of the turbulence spectrum measurement cannot be greater than the combined accuracies of this prediction and the spectral estimate.

A more direct method, not requiring a prediction of the ambiguity, of using the cross-correlated velocity signals from two laser–Doppler velocimeter sample volumes has been investigated by Clark (1970) and by van Maanen, van der Molen & Blom (1975). Use of this procedure with the ultrasonic Doppler velocimeter seems very promising. A major obstacle in using the two-sample-volume method with the laser–Doppler velocimeter is the complex alignment of the laser optics to define the two-beam intersection. Fortunately, in a pulsed Doppler velocimeter, two sample volumes may be established on a single acoustic beam in a relatively simple manner. The mixer output is applied to two sampling circuits. Both circuits sample at the pulse repetition frequency $1/\tau_{\mathrm{rp}}$, but differ slightly in phase. The resulting Doppler signals correspond to measurements from two sample volumes, separated in space (McLeod 1973). The relative positions of the sample volumes are therefore fixed electronically, and the only alignment necessary is that of the single ultrasonic beam.

The technique can be outlined as follows. Two closely spaced but non-overlapping sample volumes are placed in the flow at the desired observation point. The detected velocity signals from each are represented by

$$\omega_{\mathrm{d}\alpha}(t) = k\langle u_1\rangle_\alpha(t) + \dot{\Phi}_\alpha(t), \quad \omega_{\mathrm{d}\beta}(t) = k\langle u_1\rangle_\beta(t) + \dot{\Phi}_\beta(t), \tag{3.1}$$

where α and β denote the locations. Cross-correlating these two time signals yields

$$\overline{\omega_{\mathrm{d}\alpha}(t)\,\omega_{\mathrm{d}\beta}(t+\tau)} = \overline{k^2\langle u_1\rangle_\alpha(t)\,\langle u_1\rangle_\beta(t+\tau)} + \overline{k\langle u_1\rangle_\alpha(t)\,\dot{\Phi}_\beta(t+\tau)} + \overline{k\langle u_1\rangle_\beta(t+\tau)\,\dot{\Phi}_\alpha(t)} + \overline{\dot{\Phi}_\alpha(t)\,\dot{\Phi}_\beta(t+\tau)}. \tag{3.2}$$

As in § 2.3, the spatial-average velocity and the ambiguity processes are uncorrelated. Therefore the second and third terms of (3.2) are zero. If the two sample volumes contain different particle populations then the cross-correlation of the two ambiguity processes will be zero. Also, if the sample volumes are sufficiently close together the cross-correlation of the signals from the two sample volumes approximates the auto-correlation of the velocity at the observation point. The resulting cross-spectrum will be an estimate of the one-dimensional energy auto-spectrum, but will not contain the ambiguity component.

There are, however, several considerations in using this method with the ultrasonic Doppler velocimeter. First, it may be necessary to overlap the sample volumes partially to avoid distortion of the velocity spectrum. To the extent of this overlap, the ambiguity processes of the two sample volumes are fractionally correlated. Therefore some ambiguity components will still be present in the spectra. Also, if one sample volume lies 'in the shadow' of the other with respect to the mean flow, a portion of the particle population travels virtually unchanged from one sample volume to the other (see figure 7). Again, this will cause a partial correlation of the ambiguity processes.

On the other hand, if the sample volumes are too far apart, the cross-correlation deviates radically from the desired velocity correlation. The quantity that we seek to measure is the correlation between a velocity component at two different points

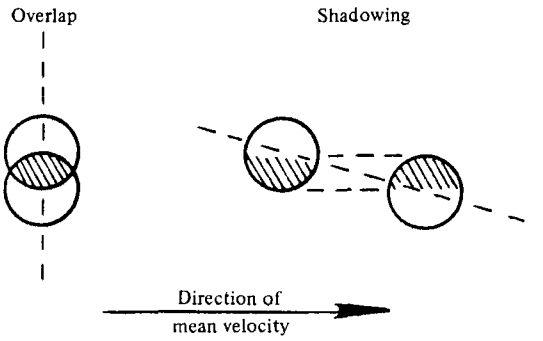

FIGURE 7. The conditions of overlap and shadowing of the sample volumes in the dual-sample-volume method.

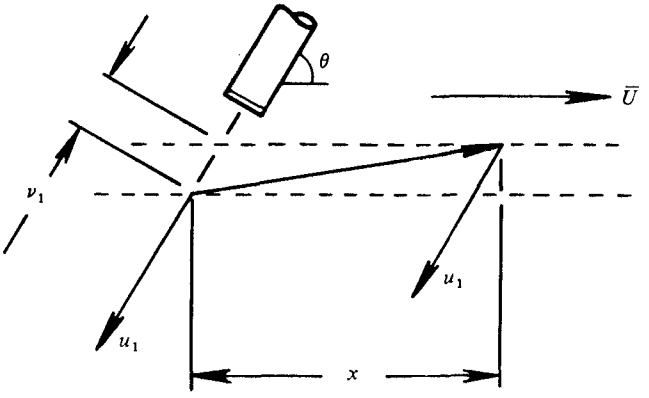

FIGURE 8. Two-point correlation.

separated by a distance r along a line parallel to the mean-flow direction (see figure 6). When the cross-correlation of the detected velocity is computed for two spatially separated sample volumes the result, according to Taylor's hypothesis (see § 2.4), is that shown in figure 8. In other words, the two measured points are not located along the mean-flow direction. This causes distortion of the correlation function, as shown at low absolute values of the time shift τ. In turn, this results in added attenuation of the energy spectrum at high wavenumbers.

For the case of isotropic turbulence, momentarily neglecting the effects of sample-volume spatial averaging, the cross-correlation of the velocities for separated sample volumes implied by figure 8 can be determined:

$$P_{11}(x) = f((x^2+\nu_1^2\sin^2\theta)^{\frac{1}{2}})\cos^2\left[\theta-\arctan\frac{\nu_1\sin\theta}{x}\right] + g((x^2+\nu_1^2\sin^2\theta)^{\frac{1}{2}})\sin^2\left[\theta-\arctan\frac{\nu_1\sin\theta}{x}\right], \quad (3.3)$$

where $f(r)$ and $g(r)$ are the actual longitudinal and transverse correlation functions, x is the separation of the sample volumes in the direction of mean flow, θ is the Doppler angle, and ν_1 is the distance of separation of the sample volumes along the beam axis.

The corresponding spectrum is determined from the Fourier transform of this equation for known functions $f(r)$ and $g(r)$.

In addition, if the sample volumes are placed on a line that is approximately perpendicular to the direction of mean velocity, in an attempt to reduce the shadow effect, the average velocity in the direction of the transducer is nearly zero. This results in very low Doppler-frequency shifts. For reasons associated with the nature of the signal-processing circuits, low-frequency components are usually lost.

Optimization of the system configuration with respect to these compromises clearly requires a knowledge of the extent to which the Doppler ambiguity is reduced as a function of the sample volume overlap and shadowing. That is, it is necessary to evaluate the spectrum associated with the autocorrelation in the fourth term of (3.2):

$$S_{\alpha\beta}(\omega) = \int_{-\infty}^{+\infty} \overline{\Phi_\alpha(t)\,\Phi_\beta(t+\tau)}\, e^{-i\omega\tau}\, d\tau. \tag{3.4}$$

This function has been derived by Garbini (1978) under the same assumptions stated in § 2.1. Briefly, the cross-correlation function may be obtained in a manner similar to the derivation of the autocorrelation made by Rice (1949), which was referred to in § 2.3. This results in

$$\overline{\Phi_\alpha(t)\,\Phi_\beta(t+\tau)} = \frac{\dot{g}^2_{\alpha\beta}(\tau) - g_{\alpha\beta}(\tau)\,\ddot{g}_{\alpha\beta}(\tau)}{2g^2_{\alpha\beta}(\tau)} \ln\left(1 - g^2_{\alpha\beta}(\tau)\right), \tag{3.5}$$

where $g_{\alpha\beta}(t)$ is the cross-correlation coefficient of $A(t)$ evaluated with sample volumes located at the two positions α and β. That is

$$g_{\alpha\beta}(\tau) = \frac{E[A_\alpha(t)\,A_\beta(t+\tau)]}{E[A_\alpha(0)\,A_\beta(0)]}. \tag{3.6}$$

The functions $A(t)$ and Φ are defined respectively in (2.11) and (2.12).

For the specific case of two sample volumes with Gaussian-shaped sample-volume directivity functions and centre-to-centre separation of (ν_1, ν_2, ν_3), the cross-correlation coefficient can be shown to be

$$g_{\alpha\beta}(\tau) = \exp\left[-\tfrac{1}{2}k^2\overline{\Delta u_1'^2}\tau^2 + \sum_{i=1}^{3} \frac{(\overline{\langle u_i\rangle} + \nu_i)^2}{4\sigma_i^2}\right]. \tag{3.7}$$

For the pulsed Doppler velocimeter in which the sample volumes are spaced electronically along the acoustic beam, ν_2 and ν_3 are zero. Notice that, when ν_1 is also zero, the result reduces to the expression for the autocorrelation coefficient of $A(t)$ discussed in § 2.3. From the Fourier transform of (3.5), the cross-spectrum is computed:

$$S_{\alpha\beta}(\omega) = \tfrac{1}{2}\pi^{\frac{1}{2}} u\, e^{-i\omega v/u^2} \sum_{n=1}^{\infty} e^{-2nw} n^{-\frac{3}{2}} \exp\left(-\frac{\omega^2 - 4n^2v^2}{4nu^2}\right), \tag{3.8}$$

where

$$u^2 = k^2\overline{\Delta u'^2} + \frac{\overline{\langle u_1\rangle^2}}{2\sigma_1^2} + \frac{\overline{\langle u_2\rangle^2}}{2\sigma_2^2} + \frac{\overline{\langle u_3\rangle^2}}{2\sigma_3^2},$$

$$v = \frac{\overline{\langle u_1\rangle}\,\nu_1}{2\sigma_1^2}, \quad w = \frac{\nu_1^2}{4\sigma_1^2}.$$

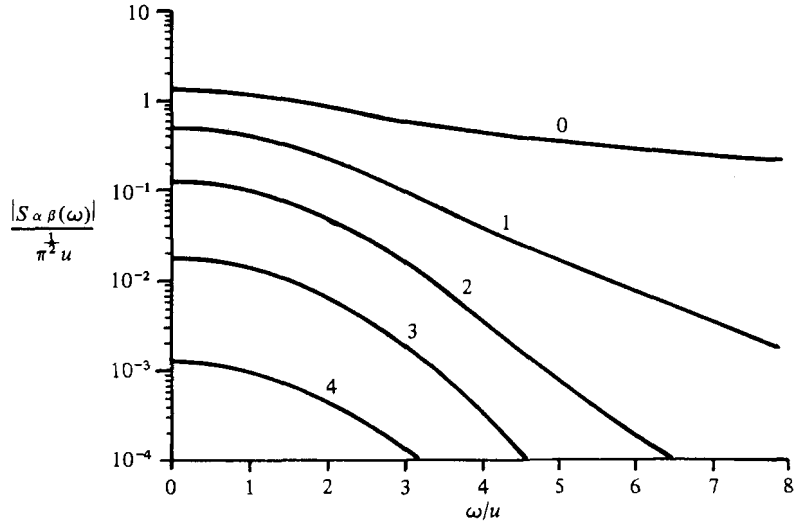

FIGURE 9. Effect of sample-volume spacing on ambiguity reduction for Doppler angle = 60° and overlap ratio = 0, 1, 2, 3, 4.

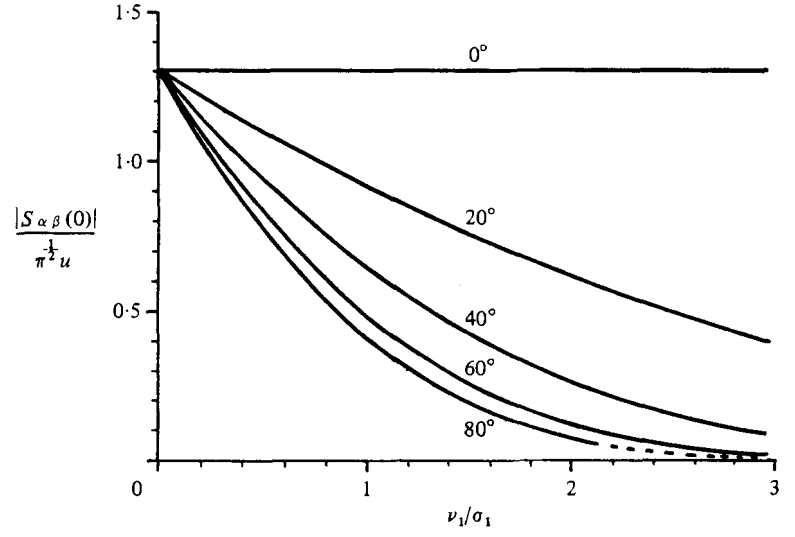

FIGURE 10. Effect of the Doppler angle on ambiguity reduction for Doppler angle = 0°, 20°, 40°, 60°, 80°.

In figure 9 the normalized magnitude of the theoretical cross-spectrum from (3.8) is plotted. This illustrates the reduction in the ambiguity for the situation in which two spherically symmetric sample volumes are positioned with normalized separation ν_1/σ_1 and with fixed angle between the beam and the direction of mean flow equal to 60°. Even for the small separation of $\nu_1/\sigma_1 = 1$, which corresponds to substantial overlap of the sample volumes, the value of the ambiguity at $\omega = 0$ is reduced by a factor of slightly less than two. Notice that the bandwidth, as well as the amplitude, of the ambiguity spectrum is decreased at larger sample-volume separations.

Conversely, the effect of shadowing on the ambiguity reduction is seen in figure 10, where the normalized magnitude of the cross-spectrum at $\omega = 0$ is plotted for various values of the Doppler angle. It should be noted that Doppler angles greater than 75° are generally impractical.

4. Conclusions

A three-dimensional stochastic model of the pulsed ultrasonic Doppler velocimeter has been represented in detail. The analysis predicts the correlation and spectral functions of the Doppler and the detected velocity signals. Explicit results are given for the case in which the sample-volume directivity is assumed to be a three-dimensional Gaussian function.

Results indicate that the turbulent intensity can be deduced from the broadening of the spectrum of the Doppler signal and a mathematical description of the effective sample volume directivity.

In the measurement of one-dimensional velocity spectra at least two major complications are identified and quantified. First, the presence of a time-varying broad-band random process (the Doppler-ambiguity process) obscures the spectrum of the random velocity. Secondly, the spatial averaging of the velocity field in the sample volume causes attenuation in the measured velocity spectrum. These phenomena are similar to those encountered in laser and radar velocimetry. These effects are aggravated for the ultrasonic instrument due to the relatively large sample volumes and wavelengths required.

It has been shown that the influence of the Doppler ambiguity process can be reduced by the use of two electronically formed sample volumes on a single acoustic beam. The overlap and orientation of these sample volumes are major considerations. The effects of these parameters on the detected velocity spectrum have been quantified in terms of the sample volume directivity.

In part 2 of the study all of the analytical results are confronted experimentally.

This research was partially funded by the National Institute of Health through research grant number HL 07293.

REFERENCES

BAKER, D. W., JOHNSON, S. L. & STRANDNESS, D. E. 1973 Prospects for quantification of transcutaneous pulsed ultrasonic Doppler techniques in cardiology and peripheral vascular disease. In *Cardiovascular Applications of Ultrasound*, pp. 108–124.

BATCHELOR, G. K. 1949 Diffusion in a field of homogeneous turbulence. I. Eulerian analysis. *Austr. J. Sci. Res.* A **2**, 437–450.

BERMAN, W. S. & DUNNING, J. W. 1973 Pipe flow measurements of turbulence and ambiguity using laser–Doppler velocimetry. *J. Fluid Mech.* **61**, 289–299.

BRODY, W. R. & MEINDLE, J. D. 1974 Theoretical analysis of the Doppler ultrasonic flowmeter. *I.E.E.E. Trans. Biomed. Engng* BME **12**, 183–192.

CLARK, W. H. 1970 Measurement of two-point correlations in a pipe using laser velocimeters. Ph.D. thesis, Dept of Aerospace Engng, University of Virginia, Charlottesville.

DURRANI, T. S. & GREATED, C. A. 1973 Statistical analysis and computer simulation of laser Doppler velocimeter systems. *I.E.E.E. Trans. Instrum. & Measurement* IM **22**, 23–34.

EDWARDS, R. V. & ANGUS, J. C. 1971 Spectral analysis of the signal from the laser Doppler flowmeter: time independent systems. *J. Appl. Phys.* **42**, 837–850.

FLAX, S. W., WEBSTER, J. G. & STUART, J. W. 1971 Statistical evaluation of the Doppler ultrasonic blood flow meter. *I.S.A. Trans.* **10**, 1–20.

FORSTER, F. K., GARBINI, J. L. & JORGENSEN, J. E. 1976 Hemodynamic turbulence measurement using ultrasonic techniques. In *Proc. 4th Ann. New England Bioengng Conf., New Haven, Conn.* (ed. S. Saha), pp. 1223–1226. Pergamon.

GARBINI, J. L. 1978 Measurement of fluid turbulence based on pulsed ultrasound techniques. Ph.D. dissertation. Dept Mechanical Engng, Univ. Washington, Seattle.

GARBINI, J. L., FORSTER, F. K. & JORGENSEN, J. E. 1982 Measurement of fluid turbulence based on pulsed ultrasound techniques. Part 2. Experimental investigation. *J. Fluid Mech.* **118**, 471–505.

GEORGE, W. K. & LUMLEY, J. L. 1973 The laser–Doppler velocimeter and its application to the measurement of turbulence. *J. Fluid Mech.* **60**, 321–363.

JORGENSEN, J. E. & GARBINI, J. L. 1974 An ultrasonic procedure of calibration for the pulsed ultrasonic Doppler flowmeter. *Trans. A.S.M.E.* I, *J. Fluids Engng* **96**, 158–167.

LAUFER, J. 1954 *The structure of turbulence in fully-developed pipe flow. NACA Rep.* no. 1174.

LAWSON, J. L. & ULENBECH, G. E. 1950 *Threshold Signals*, p. 369. MIT Press.

VAN MAANEN, H. R. E., VAN DER MOLEN, J. B. & BLOM, J. 1975 Reduction of ambiguity noise in laser–Doppler velocimetry by a cross correlation technique. In *The Accuracy of Flow Measurements by Laser Doppler Methods: Proc. LDA Symp., Technical University of Denmark* (ed. P. Buchhave), pp. 81–88. Hemisphere.

MCLEOD, F. D. 1973 Multichannel pulse Doppler techniques: cardiovascular applications of ultrasound. In *Proc. Int. Symp. held at Janssen Pharmaceutica, Beerse, Belgium* (ed. R. Reneman), pp. 85–107. North-Holland.

MIDDLETON, D. 1950 Spectrum of frequency-modulated waves. *Quart. Appl. Math.* **8**, 59–81.

NEWHOUSE, V. L. 1973 Transit time broading in ultrasonic Doppler flow measurement systems. *Purdue University School of Elec. Engng Int. Rep.*

NEWHOUSE, V. L., VARNER, W. V. & BENDICK, P. J. 1977 Geometrical spectrum broadening in ultrasonic Doppler systems. *I.E.E.E. Trans. Biomed. Engng* BME **24**, 478–480.

PAO, YHI-HO 1965 Structure of turbulent velocity and scalar fields at large wave numbers. *Phys. Fluids* **8**, 1063–1075.

RICE, S. O. 1945 Mathematical analysis of random noise. *Bell. Syst. Tech. J.* **24**, 46–159.

RICE, S. O. 1949 Statistical properties of a sine wave plus random noise. *Bell Syst. Tech. J.* **27**, 109–157.

ROGERS, R. R. & TRIPP, B. R. 1964 Some radar measurements of turbulence in snow. *J. Appl. Met.* **3**, 603–610.

SRIVASTAVA, R. C. & ATLAS, D. 1974 Effect of finite radar pulse volume on turbulence measurements. *J. Appl. Met.* **13**, 472–480.

SYCHRA, J. 1972*a* Inverse problem in the theory of turbulence filtering by the radar pulse volume. *Preprints of 15th Radar Met. Conf., Urbana*, pp. 285–291. American Met. Soc.

SYCHRA, J. 1972*b* *On the Theory of Pulse-Volume filtering of the Turbulence Reflectivity and Velocity Fields.* Lab. for Atmos. Probing, Dept Geophys. Sci., University of Chicago.